

# UC Irvine

## UC Irvine Previously Published Works

### Title

Noninvasive blood flow imaging for real-time feedback during laser therapy of port wine stain birthmarks.

### Permalink

<https://escholarship.org/uc/item/19f084t6>

### Journal

Lasers in surgery and medicine, 40(3)

### ISSN

0196-8092

### Authors

Huang, Yu-Chih  
Ringold, Tyson L  
Nelson, J Stuart  
[et al.](#)

### Publication Date

2008-03-01

### DOI

10.1002/lsm.20619

### Copyright Information

This work is made available under the terms of a Creative Commons Attribution License, available at <https://creativecommons.org/licenses/by/4.0/>

Peer reviewed



Published in final edited form as:

*Lasers Surg Med.* 2008 March ; 40(3): 167–173. doi:10.1002/lsm.20619.

## Noninvasive Blood Flow Imaging for Real-Time Feedback During Laser Therapy of Port Wine Stain Birthmarks

Yu-Chih Huang, MS<sup>1,2</sup>, Tyson L. Ringold<sup>1,3</sup>, J. Stuart Nelson, MD, PhD<sup>1,4</sup>, and Bernard Choi, PhD<sup>1,4,\*</sup>

<sup>1</sup>Beckman Laser Institute and Medical Clinic, University of California, Irvine, California 92612

<sup>2</sup>Department of Electrical Engineering and Computer Science, University of California, Irvine, California 92697

<sup>3</sup>Department of Mechanical Engineering, University of California, Los Angeles, California 90095

<sup>4</sup>Department of Biomedical Engineering, University of California, Irvine, California 92697

### Abstract

**Background and Objectives**—During laser therapy of port wine stain (PWS) birthmarks, regions of persistent perfusion may exist. Immediate retreatment of such regions may improve PWS laser therapeutic outcome. To address this need, we propose use of laser speckle imaging (LSI) to provide real-time, quantitative feedback during laser surgery. Herein, we present in vitro and in vivo data collected with a clinic-based LSI instrument.

**Study Design/Materials and Methods**—Prior to clinical implementation, we first investigated three aspects of LSI deemed important for clinical imaging: (1) instrument depth of field (DOF); (2) effects of laser irradiance on speckle flow index (SFI) values; and (3) measurement repeatability. Clinical measurements were acquired from the lesions of PWS patients immediately prior to and after laser therapy at the Beckman Laser Institute.

**Results**—Our preclinical data suggest the following: (1) instrument DOF was ~1 cm; (2) quantitative flow characterization with LSI was practically unaffected at normalized irradiance values between 0.06 and 0.5; and (3) our LSI instrument was capable of highly reproducible SFI values. From our clinical measurements, we found that the relative difference between blood perfusion in PWS lesions and adjacent normal skin was highly variable. Based on SFI images, the perfusion of PWS skin is sometimes indistinguishable from that of adjacent normal skin. With laser therapy, we measured a global decrease in blood perfusion, and we frequently observed distinct regions of persistent perfusion.

**Conclusions**—Our results demonstrate the potential role of image-guided laser therapy of PWS birthmarks. LSI is a promising tool for noninvasive blood flow characterization during laser therapy due to its relative simplicity and low cost. *Lasers Surg.*

### Keywords

port wine stain; laser speckle imaging; laser Doppler flowmetry; noninvasive blood flow imaging; laser therapy; vascular birthmarks

\*Correspondence to: Bernard Choi, PhD, Beckman Laser Institute and Medical Clinic, University of California, Irvine, 1002 Health Sciences Road East, Irvine, CA 92612. E-mail: E-mail: choib@uci.edu.

## INTRODUCTION

Port wine stain (PWS) birthmarks are progressive vascular malformations that occur in ~12,000 live births per year in the United States. The majority (~90%) of PWS birthmarks occurs on the head and neck and, thus, are difficult to conceal [1]. As a result, personality development is adversely influenced in virtually all patients by the negative reaction of others to a “marked” person [2]. Sturge-Weber syndrome (encephalotrigeminal angiomatosis), which is commonly found among those patients with PWS involving the distribution of the first branch of the trigeminal nerve is associated with increased incidence of glaucoma and seizures. The cause and origin of PWS remains incompletely understood. The most likely hypothesis for the development of PWS is the deficiency or absence of surrounding neurons regulating blood flow through the ectatic post-capillary venules. As a result, the blood vessels are unable to constrict normally and remain permanently dilated. Progressive development of the PWS results in a darker appearance, soft tissue hypertrophy, nodularity, and overall further disfigurement [3].

Current treatment options have significant limitations in terms of efficacy and risk [4]. With laser therapy, a reduction in size and degree of redness of PWS skin occurs in ~60% of patients. After ten treatment sessions, complete disappearance of the PWS occurs in only ~10% of patients [5]. To reduce the financial burden and potential risks of repeated treatments under general anesthesia, there is a need for innovative, individualized methods to maximize the reduction in PWS redness per treatment session. Without addressing this need, the overall efficacy of PWS laser therapy will remain variable because treatment protocols will remain based primarily on the subjective impression and overall experience of the clinician.

To address this need, we set out to develop a noninvasive, objective method to characterize PWS skin blood flow changes during laser surgery. Laser Doppler flowmetry and laser Doppler imaging, both established methods in studies of microvascular skin characterization, are limited by the need for mechanical scanning of the probe laser beam, resulting in long (on the order of minute) image collection times. We instead propose use of laser speckle imaging (LSI) [6-9] to provide real-time, quantitative feedback during laser surgery. LSI relies on acquisition and analysis of a single image captured at an exposure time that is considerably longer than a characteristic correlation time associated with the fluctuation frequency. A faster blood flow appears more blurred in the captured image than regions of slower or no flow. The degree of blurring is quantified as the local speckle contrast value, with zero contrast representing no speckle and hence high blood flow, and unity contrast representing a fully developed speckle pattern and hence no flow.

Herein, we present *in vitro* and *in vivo* data collected with a clinic-based LSI instrument. Collectively, the data suggest the potential of LSI to serve as an intraoperative imaging tool to furnish clinicians with real-time images of blood perfusion.

## MATERIALS AND METHODS

### Clinical LSI Instrument

To facilitate studies involving human subjects, we engineered a clinic-based LSI instrument (Fig. 1). A primary design consideration was to collect raw speckle images with subjects positioned as comfortably as possible. To this end, an articulated arm was used as the base platform to provide flexibility in instrument positioning. Continuous-wave light emitted from a 633-nm HeNe laser ( $P = 30$  mW, Edmund Industrial Optics, Barrington, NJ) was delivered to the target area with an optical fiber and diffusion glass. We selected this method for beam expansion over a diverging lens because of the higher degree of homogeneity within the irradiated field that could be achieved at a comparable speckle contrast (unpublished data).

Raw speckle reflectance images were collected with a 12-bit, thermoelectrically cooled CCD camera (Retiga 2000R, QImaging, Burnaby, BC, Canada) with a sensor size of 1600×1200 (H×V) pixels. Image data were transferred via FireWire connection to a PC for storage, processing, and visualization. Custom written LabVIEW software (Version 8.0, National Instruments, Austin, TX) was used to control all aspects of image acquisition and processing. With a macro lens (Edmund Industrial Optics) attached to the camera, the size of the imaging area was 4 cm×3 cm.

### Speckle Image Processing

To extract blood flow information from the raw speckle images, we evaluated local spatial intensity variations in the speckle pattern. In this study, a sliding window of 7×7 pixels was used to convert the recorded images to speckle contrast images. The speckle contrast  $K$  is typically defined as the ratio of the standard deviation  $\sigma$  to the mean intensity  $\langle I \rangle$  and is between 0 and 1 [10]. When  $K$  is equal to 0, the speckle pattern is completely blurred by the relatively large motion of flowing optical scatterers such as red blood cells. When  $K$  is equal to 1, the speckle pattern is fully developed. At each image subregion defined by the sliding window position, the  $K$  value of the center pixel is computed as

$$K = \frac{\sigma}{\langle I \rangle} \quad (1)$$

Assuming a Lorentzian flow velocity distribution [11], the following speckle imaging equation can be derived:

$$K = \left[ \left( \frac{\tau_c}{2T} \right) \left\{ 1 - \exp \left( \frac{-2T}{\tau_c} \right) \right\} \right]^{1/2} \quad (2)$$

where  $\tau_c$  the correlation time and  $T$  is the camera integration time. The relative blood flow is equivalent to the inverse of the correlation time ( $1/\tau_c$ ) and, thus, a speckle flow index (SFI) map is computed. For this study, we set the value of  $T$  to 10 milliseconds which was selected based on flow phantom experiments performed previously [7].

### Preclinical Characterization of LSI Instrument

We first investigated three aspects of LSI that we deemed as important for clinical imaging: (1) instrument depth of field (DOF), (2) effects of laser irradiance on SFI values, and (3) measurement repeatability.

**Depth of field (DOF)**—Speckle contrast values are considerably affected by the location of the imaging plane relative to the focal plane. For clinical imaging of PWS birthmarks, we anticipated that skin curvature and variable soft tissue hypertrophy would require that our LSI instrument has a relatively large DOF. To characterize the DOF of our instrument, we acquired raw speckle images of an aluminum block. The block was positioned at various longitudinal positions away from the focal plane. Speckle contrast maps were extracted from the raw speckle images, and a mean and standard deviation of the  $K$  values per map were computed.

**Effects of laser irradiance on SFI values**—In the absence of noise due to instrumentation or experimental conditions, values of  $K$  are not affected by laser irradiance as long as the spatial distribution is uniform within the imaging field of view. In practice, we anticipated that  $K$  values would be affected at both near saturation and relatively low irradiances due to nonlinearities in camera performance and instrument noise. Due to the multiple factors that are

expected to affect ultimately imaging performance, we performed experiments to determine empirically the range of irradiance values over which SFI values are unaffected by irradiance. To achieve this goal, we acquired raw speckle images of the subdermal microvascular network of a mouse dorsal window chamber [6,7]. The independent variable was laser irradiance, and the dependent variable was the mean SFI value extracted from a predefined site (Fig. 2). The Institutional Animal Care and Use Committee at the University of California, Irvine, approved these experiments.

**Measurement repeatability**—For reliable clinical imaging, the measurements must be repeatable. To evaluate the repeatability of our blood flow measurements, we acquired raw speckle reflectance images from four human subjects. All imaged regions consisted of visibly normal skin. For each subject, we acquired two sets of speckle images: one from the arm and the other from the face. Afterwards, each subject was allowed to move freely for 3 minutes after which the instrument was repositioned, and images from the same two regions were acquired a second time. Offline, the images were converted to SFI images and mean SFI values extracted from the predefined sites.

### Clinical LSI of PWS Subjects

We have acquired images from patients undergoing laser therapy of PWS birthmarks at the Beckman Laser Institute and Medical Clinic. The measurement protocol has been approved by the human subjects Institutional Review Board at University of California, Irvine. Prior to acquisition of clinical measurements, each subject reviewed and signed an informed consent form. Herein, we present representative data acquired from a Caucasian female subject with a PWS birthmark on the left face in the V2 dermatomal distribution. The PWS skin was treated with a V-Beam Perfecta pulsed dye laser (PDL,  $\lambda=595$  nm, Candela Corp., Wayland, MA) at a radiant exposure of  $10 \text{ J/cm}^2$ ; pulse durations of 1.5, 10, and 20 milliseconds; and a treatment spot size of 10 mm. Prior to each laser pulse, a 30 milliseconds cryogen spurt was applied with a 30 milliseconds delay between the end of the spurt and onset of the laser pulse.

Raw speckle images were acquired before and immediately after laser therapy. The camera was focused on the target area at a working distance of  $\sim 300$  mm. To perform proper sampling of the speckle pattern, the f-stop of the macro lens was set to match the speckle size to the pixel pitch ( $7.4 \mu\text{m}$ ) of the CCD camera. The speckle size is equal to the width of the diffraction-limited spot and is given by  $2.44 \lambda f/\#$ , where  $\lambda$  is the laser wavelength (633 nm). After positioning the camera, a sequence of ten raw speckle images (10 milliseconds exposure time per image) was collected and the SFI images computed during post processing. The total time required for positioning the camera and acquiring an image sequence was  $\sim 5$  minutes.

## RESULTS

### Depth of Field (DOF)

To study DOF, raw speckle images were acquired from an aluminum block at different longitudinal positions with respect to the camera. At a relative focal distance of zero (i.e., best focus), mean speckle contrast was 0.75 (Fig. 3). At a relative focal distance of  $\pm 0.5$  cm, mean speckle contrast was 0.755, an increase of only 0.6%. However, at a relative focal distance of  $\pm 0.1$  cm, mean speckle contrast decreased by 10-21%. Collectively, our data demonstrate that for our clinical LSI instrument, the DOF is  $\sim 1$  cm.

## A Wide Range of Laser Irradiance Values can be Used for LSI With a Negligible Effect on SFI Values

We defined the normalized irradiance such that a value of unity corresponded to near-saturation reflectance imaging. Our data (Fig. 4) demonstrate that quantitative flow characterization with LSI is practically unaffected at normalized irradiance values between 0.06 and 0.5.

## Quantitative SFI Data Demonstrate Repeatability of LSI Measurements

From qualitative analysis of acquired pairs of SFI images before and after LSI instrument repositioning, we noted a high degree of similarity between the images (Fig. 5). Collectively, the SFI values showed minimal changes after instrument repositioning (Fig. 6) demonstrating the stability of our LSI instrument. Although the change in mean SFI value for each replicate measurement was significantly different ( $P < 0.01$ ), the difference in values was on average less than 3%, suggesting that the measurements are fairly repeatable. These findings are important for clinical implementation of LSI because they suggest that measurable changes in SFI values acquired prior to and immediately after laser therapy are due to the treatment itself and not systematic errors associated with imaging methodology.

## Images of Regions of Persistent Perfusion After Laser PWS Therapy

Raw speckle images were acquired from a PWS skin predefined site enclosed within the black line (Fig. 7) prior to and 15 minutes after laser therapy. Prior to treatment (Fig. 7A), the blood flow distribution was fairly heterogeneous. After treatment (Fig. 7B), blood flow decreased presumably due to PWS blood vessel photocoagulation. Collectively, these data confirmed that regions of persistent perfusion remain immediately after laser therapy.

## Images of Complete Reduction of PWS Blood Perfusion After Laser PWS Therapy

After 10 weeks, we acquired a second set of raw speckle images from the same subject shown in Figure 7. Raw speckle images were acquired from the marked predefined site (Fig. 8) containing both normal and PWS skin areas (boundary denoted with dashed line). Prior to therapy, we observed that the mean blood perfusion in the PWS area was higher as compared to normal skin (Fig. 8B). Fifteen minutes after laser therapy, the PWS skin area became darker (Fig. 8C) due to purpura formation, commonly used as an endpoint of PDL therapy [12]. The perfusion in the PWS area was lower overall after laser treatment whereas the perfusion in the normal skin remained unchanged. In contrast with the SFI image in Figure 7B, regions of persistent perfusion were not observed within the treated area. The boundary between the treated and non-treated areas was clearly evident.

## DISCUSSION

LSI is an optical technique capable of detecting and recording relative changes in fluid flow and might be very useful in providing a dynamic measurement of tissue blood flow. In this article, we have quantified the DOF (Fig. 3), effect of laser irradiance on SFI values (Fig. 4), and measurement repeatability (Fig. 5). Furthermore, clinical LSI has been used to identify regions of acute persistent perfusion in PWS skin after laser therapy (Fig. 7). To date, only a few studies exist in the peer-reviewed literature on the topic of blood flow in PWS vessels. The majority of these studies have involved either laser Doppler imaging [13-15] or Doppler optical coherence tomography [16-18] to assess blood flow dynamics with laser therapy. In this study, we employed LSI because of the following advantages over optical Doppler methods: cost, simplicity, and potential ease of integration into current laser systems.

Since the goal of laser therapy of vascular abnormalities is photocoagulation of the blood vessels, physicians rely on biomarkers, such as purpura formation, to indicate a desired

endpoint of PDL therapy. However, our clinical data (Fig. 7) demonstrate that persistent perfusion regions exist even after surgery by a highly skilled physician experienced in PWS laser therapy. LSI can provide a rational imaged-guided approach to assess the treatment outcome in real time and aid in identification of regions of persistent perfusion that could be retreated immediately, perhaps using different laser parameters.

In response to the first treatment session (Fig. 7), the mean SFI value decreased to 51% of its pretreatment value. The standard deviation increased 22%, most likely due to the increased heterogeneity of the skin perfusion after treatment (Fig. 7B). In response to the second treatment session performed 10 weeks later (Fig. 8), the mean SFI value decreased to 64% of its pretreatment value. The standard deviation also decreased, due to the more homogeneous perfusion reduction in response to laser therapy (Fig. 8D). A comparison of mean pretreatment SFI values from perfusion images acquired prior to each treatment session (i.e., Figs. 7A and 8C) results in a 15% increase in mean SFI values, which is an unexpected outcome. However, we believe that this outcome is not necessarily representative of the true relative change in mean SFI values. Camera view angle is expected to affect extracted SFI values. We recently observed a similar causal relationship, with camera view angle having a significant effect on skin color values extracted from facial diffuse reflectance images [19]. The images shown in Figures 7 and 8 are clearly taken with different view angles, and thus we hesitate to draw any strong conclusion from a comparison of pretreatment mean SFI values shown in these images. Future efforts will focus on studying the effect of view angle on SFI values.

It is conceivable that LSI data may be affected by changes in blood oxygenation during surgery. One visual manifestation of such changes is purpura formation. It is well known that the absorption properties of blood vary with oxygen saturation. From Monte Carlo simulations using MCML [20], we determined that complete deoxygenation of blood initially at a 75% oxygen saturation state (to simulate PWS post-capillary venules) results in a maximum expected reflectance decrease of 9% (unpublished data). Thus, the mean intensity in the denominator of Eq. (1) would decrease. However, the standard deviation is expected to similarly decrease, resulting in no overall change in speckle contrast. Thus, as a first-order approximation, changes in blood absorption properties are not expected to alter speckle contrast and, hence, SFI values. Nevertheless, a more detailed analysis of the effects of light penetration depth dynamics (due to changes in optical properties) on speckle contrast is currently underway.

Static optical scattering results in blurring of blood vessel features and reduces measured speckle contrast, and hence SFI, values [21,22]. Experimental protocols have been proposed to address this issue and ameliorates its impact [21,22] and will be the subject of future studies. In this study, we focus instead on the gross vascular response to laser therapy and in particular the presence (Fig. 7) or absence (Fig. 8) of regions of persistent perfusion. Since minimal changes to bulk skin optical scattering are expected with laser therapy, we expect that direct comparison of SFI values extracted from raw speckle image sequences taken before and after therapy is a valid approach.

## CONCLUSIONS

We have engineered and characterized a clinic-based LSI instrument for use as a surgical guidance tool. Our data suggest that our instrument has an adequately large DOF, is relatively insensitive to laser irradiance, and provides repeatable blood flow images. With laser therapy of PWS birthmarks, a heterogeneous map of perfusion has been observed with regions of persistent perfusion. Immediate retreatment of these regions may result in an improved treatment outcome per session, reducing the number of treatment sessions required for complete PWS blanching.

## ACKNOWLEDGMENTS

This research was supported in part by the A. Ward Ford Foundation (BC); Arnold and Mabel Beckman Foundation; National Institutes of Health (NIH) (JSN); NIH General Clinical Research Center (GCRC) at University of California, Irvine (BC); and NIH Laser Microbeam and Medical Program (LAMMP). We would like to express our gratitude to the following Beckman Laser Institute researchers for their assistance and insightful comments: Dr. David Cuccia and Dr. Walfre Franco, and Ms. Nadia Tran.

Contract grant sponsor: A. Ward Ford Foundation (BC); Contract grant sponsor: Arnold and Mabel Beckman Foundation; Contract grant sponsor: National Institutes of Health (NIH); Contract grant sponsor: NIH General Clinical Research Center (GCRC); Contract grant sponsor: NIH Laser Microbeam and Medical Program (LAMMP).

## REFERENCES

1. Tallman B, Tan OT, Morelli JG, Piepenbrink J, Stafford TJ, Trainor S, Weston WL. Location of port-wine stains and the likelihood of ophthalmic and or central-nervous-system complications. *Pediatrics* 1991;87(3):323–327. [PubMed: 1805804]
2. Troilius A, Wrangsjo B, Ljunggren B. Patients with port-wine stains and their psychosocial reactions after photothermolytic treatment. *Dermatol Surg* 2000;26(3):190–196. [PubMed: 10759791]
3. Ashinoff R, Geronemus RG. Capillary hemangiomas and treatment with the flash lamp-pumped pulsed dye-laser. *Arch Dermatol* 1991;127(2):202–205. [PubMed: 1990985]
4. Lanigan SW. Port-wine stains unresponsive to pulsed dye laser: Explanations and solutions. *Br J Dermat* 1998;139(2):173–177.
5. van der Horst C, Koster PHL, de Borgie C, Bossuyt PMM, van Gemert MJC. Effect of the timing of treatment of port-wine stains with the flash-lamp-pumped pulsed dye-laser. *New Engl J Med* 1998;338(15):1028–1033. [PubMed: 9535667]
6. Choi B, Kang NM, Nelson JS. Laser speckle imaging for monitoring blood flow dynamics in the in vivo rodent dorsal skin fold model. *Microvasc Res* 2004;68(2):143–146. [PubMed: 15313124]
7. Choi B, Jia WC, Channual J, Kelly KM, Lotfi J. The importance of long-term monitoring to evaluate the microvascular response to light-based therapies. *J Invest Dermatol* 2008;128:485–488. [PubMed: 17657245]
8. Forrester KR, Tulip J, Leonard C, Stewart C, Bray RC. A laser speckle imaging technique for measuring tissue perfusion. *IEEE Trans Biomed Eng* 2004;51(11):2074–2084. [PubMed: 15536909]
9. Haiying C, Qingming L, Shaoqun Z, Shangbin C, Jian C, Hui G. Modified laser speckle imaging method with improved spatial resolution. *J Biomed Opt* 2003;8(3):559–564. [PubMed: 12880364]
10. Goodman, JW. *Statistical Optics*. John Wiley & Sons, Inc; New York: 1985.
11. Fercher AF, Briers JD. Flow visualization by means of single-exposure speckle photography. *Opt Commun* 1981;37:326–329.
12. Kelly KM, Choi B, McFarlane S, Motosue A, Jung B, Khan MH, Ramirez-San-Juan JC, Nelson JS. Description and analysis of treatments for port-wine stain birthmarks. *Arch Facial Plast Surg* 2005;7(5):287–294. [PubMed: 16172335]
13. Troilius A, Wardell K, Bornmyr S, Nilsson GE, Ljunggren B. Evaluation of port wine stain perfusion by laser doppler imaging and thermography before and after argon-laser treatment. *Acta Derm Venerologica* 1992;72(1):6–10.
14. Jernbeck J, Malm M. Calcitonin gene related peptide increases the blood-flow of port-wine stains and improves continuous-wave dye-laser treatment. *Plast Reconstr Surg* 1993;91(2):245–251. [PubMed: 8430139]
15. McGill DJ, Mackay IR. The effect of ambient temperature on capillary vascular malformations. *Br J Dermatol* 2006;154(5):896–903. [PubMed: 16634893]
16. Zhao YH, Chen ZP, Saxer C, Xiang SH, de Boer JF, Nelson JS. Phase-resolved optical coherence tomography and optical Doppler tomography for imaging blood flow in human skin with fast scanning speed and high velocity sensitivity. *Opt Lett* 2000;25(2):114–116. [PubMed: 18059800]
17. Nelson JS, Kelly KM, Zhao YH, Chen ZP. Imaging blood flow in human port-wine stain in situ and in real time using optical Doppler tomography. *Arch Dermatol* 2001;137(6):741–744. [PubMed: 11405763]



18. Ren HW, Ding ZH, Zhao YH, Miao JJ, Nelson JS, Chen ZP. Phase-resolved functional optical coherence tomography: Simultaneous imaging of in situ tissue structure, blood flow velocity, standard deviation, birefringence, and Stokes vectors in human skin. *Opt Lett* 2002;27(19):1702–1704. [PubMed: 18033341]
19. Jung B, Choi B, Shin Y, Durkin AJ, Nelson JS. Determination of optimal view angles for quantitative facial image analysis. *J Biomed Opt* 2005;10(2):024002. [PubMed: 15910076]
20. Wang LH, Jacques SL, Zheng LQ. MCML—Monte-Carlo modeling of light transport in multilayered tissues. *Comput Meth Prog Biomed* 1995;47(2):131–146.
21. Zakharov P, Volker A, Buck A, Weber B, Scheffold F. Quantitative modeling of laser speckle imaging. *Opt Lett* 2006;31(23):3465–3467. [PubMed: 17099751]
22. Bandyopadhyay R, Gittings AS, Suh SS, Dixon PK, Durian DJ. Speckle-visibility spectroscopy: A tool to study time-varying dynamics. *Rev Sci Instrum* 2005;76:093110.

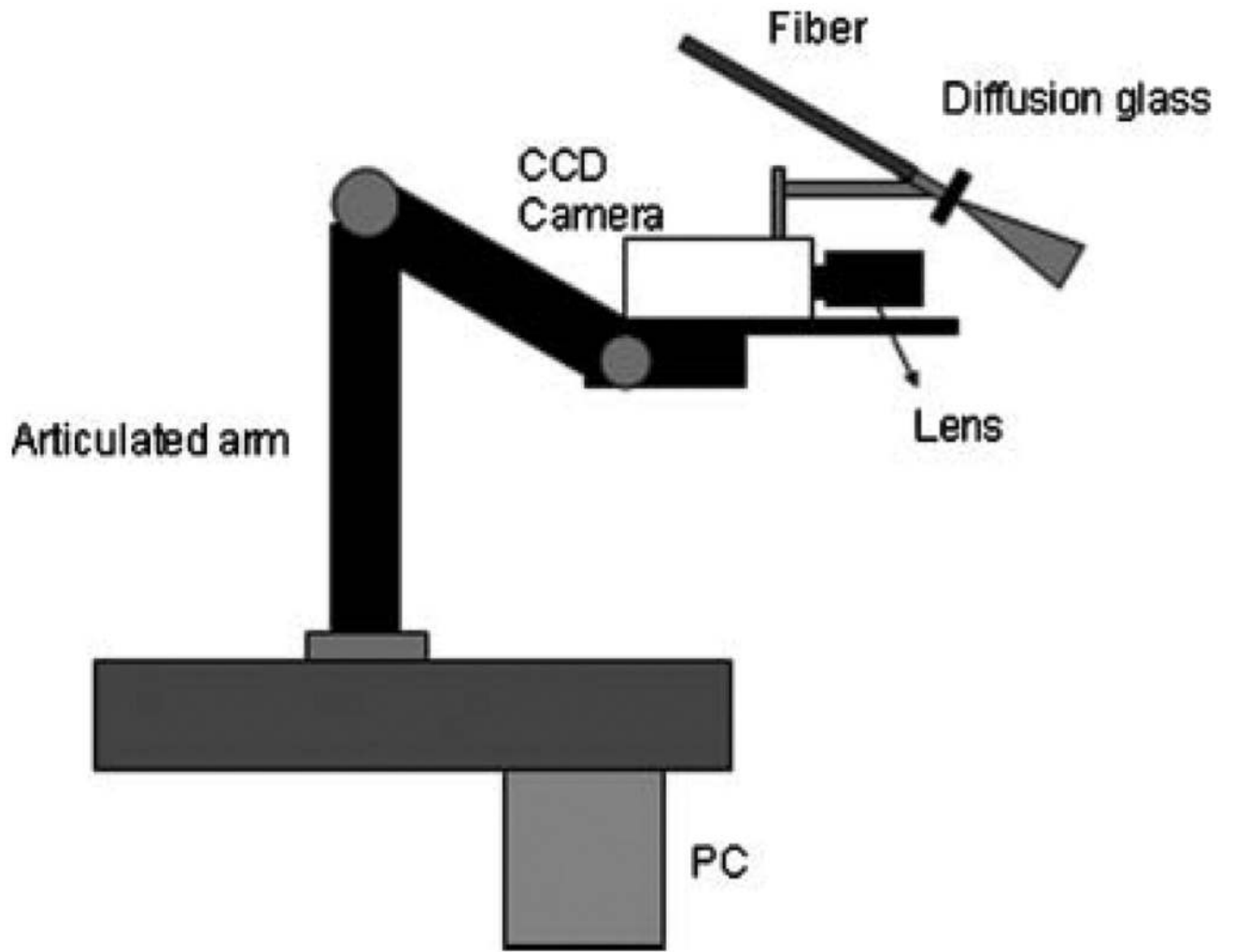


**Fig. 1.**  
Schematic of clinical LSI instrument.

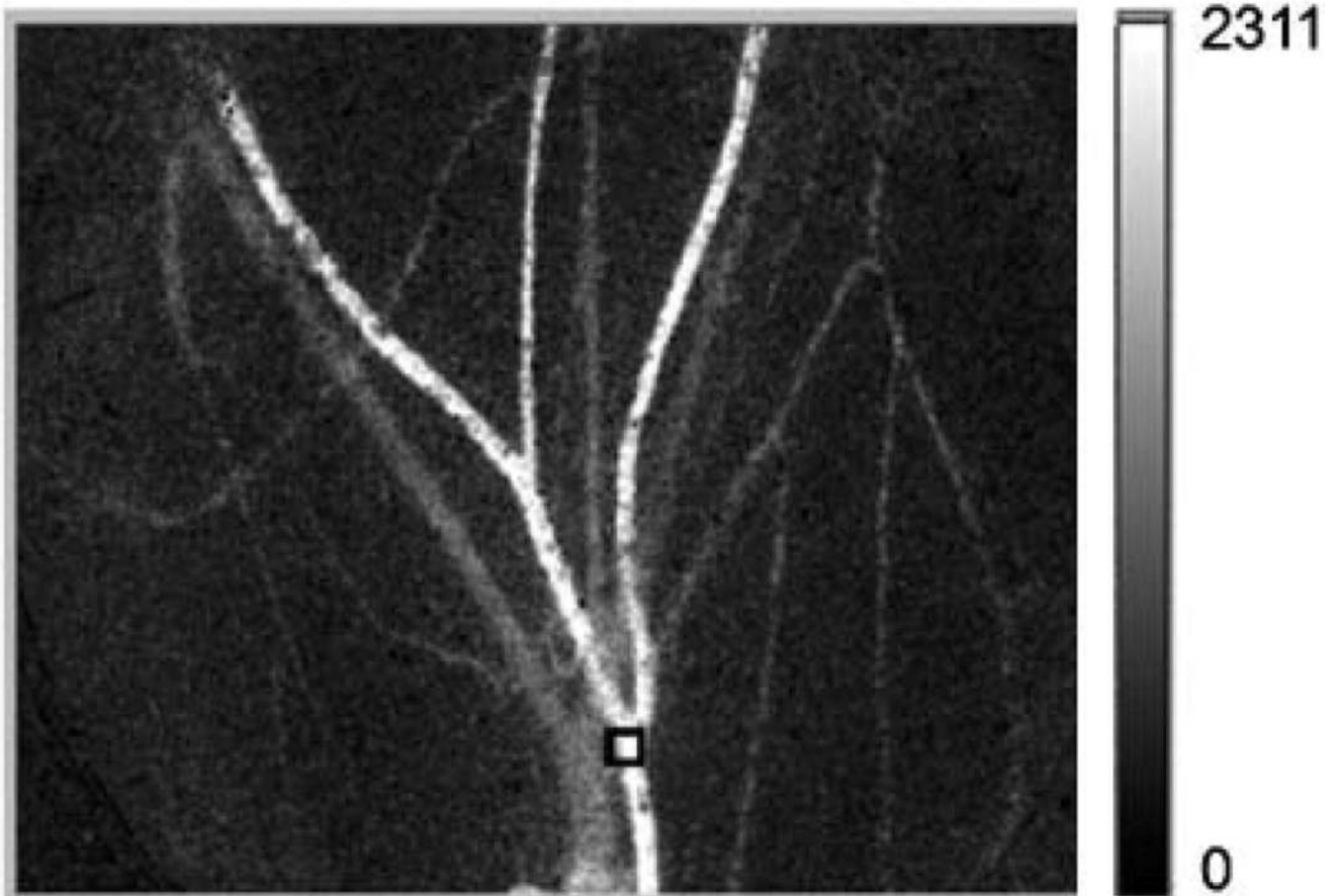


**Fig. 2.** SFI image of the mouse dorsal window chamber model used to evaluate the effect of laser irradiance on extracted SFI values. The region of interest selected for quantitative analysis is enclosed within the black square superimposed on the image.

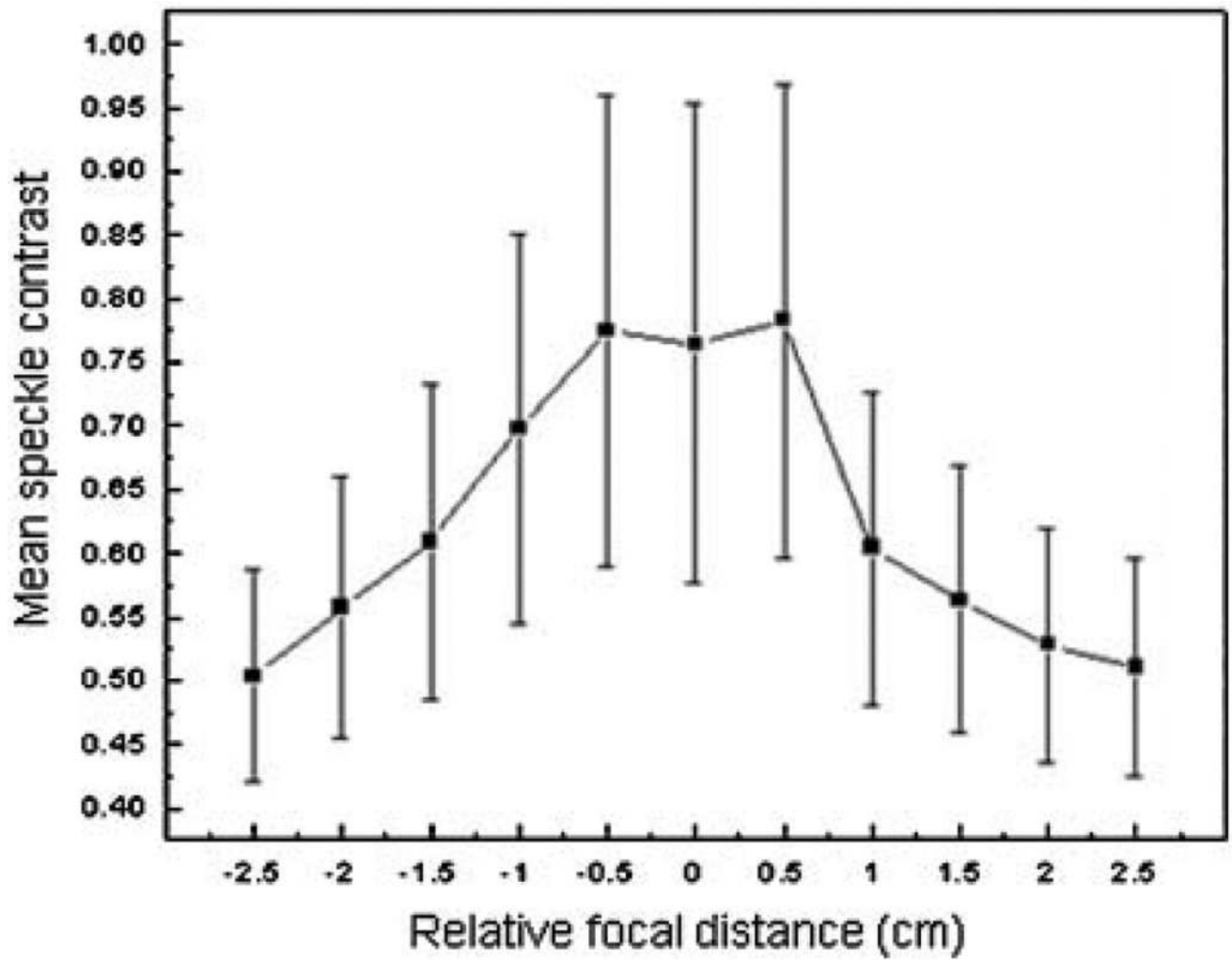


**Fig. 3.** For raw speckle images taken at a relative focal distance of  $\pm 0.5$ cm, the mean speckle contrast was similar to that at best focus (relative focal distance of 0 cm). For raw speckle images taken at relative focal distances greater than 0.5 cm from best focus, the mean speckle contrast decreased significantly ( $P < 0.01$ ). Thus, our instrument DOF was determined to be  $\sim 1$  cm. Error bars represent the standard deviation of the mean SFI value.

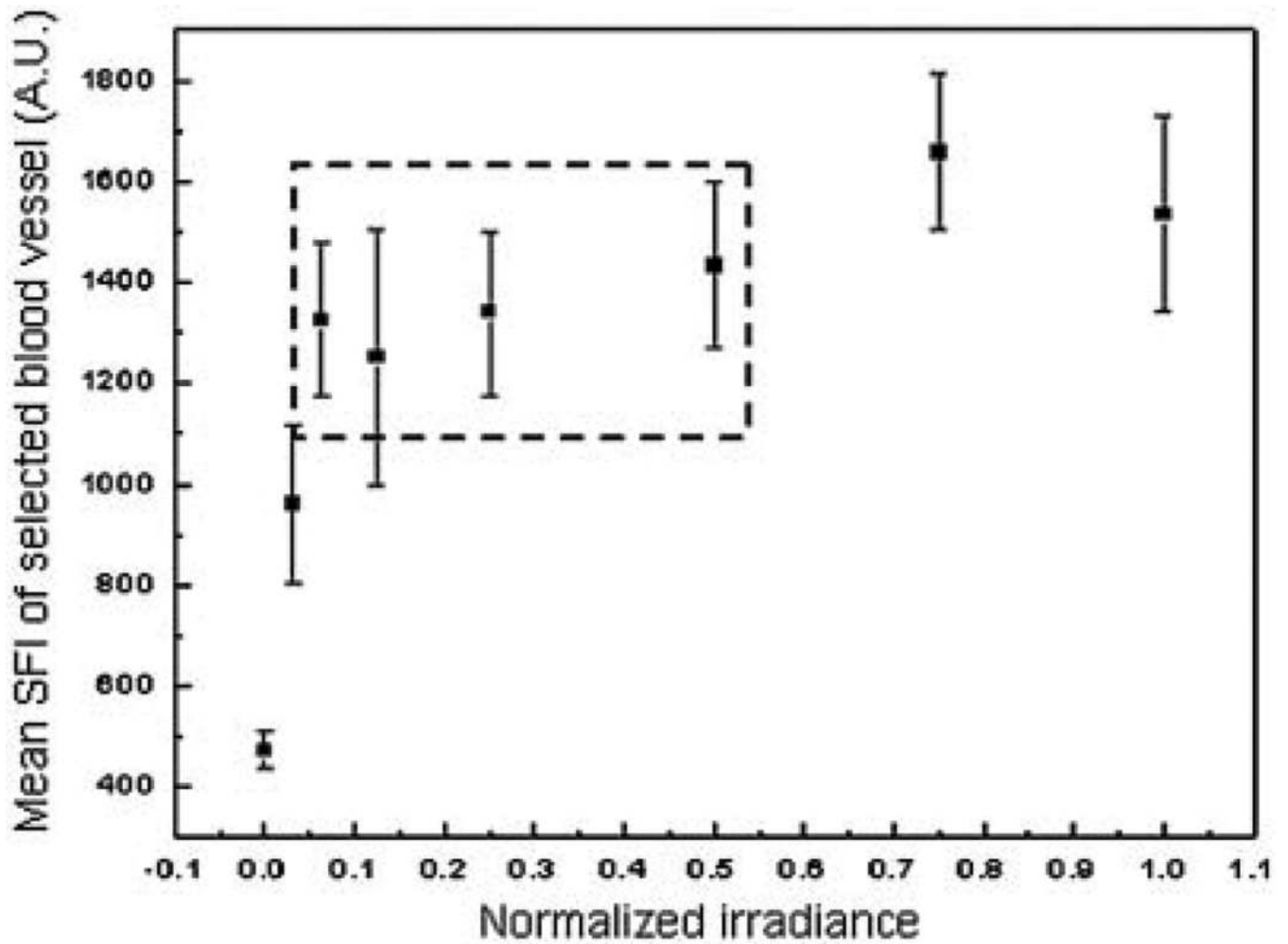


**Fig. 4.** With our clinical LSI instrument, we determined that SFI values were minimally affected by laser irradiance at normalized values between 0.06 and 0.5 (i.e., data points enclosed within dashed lines).

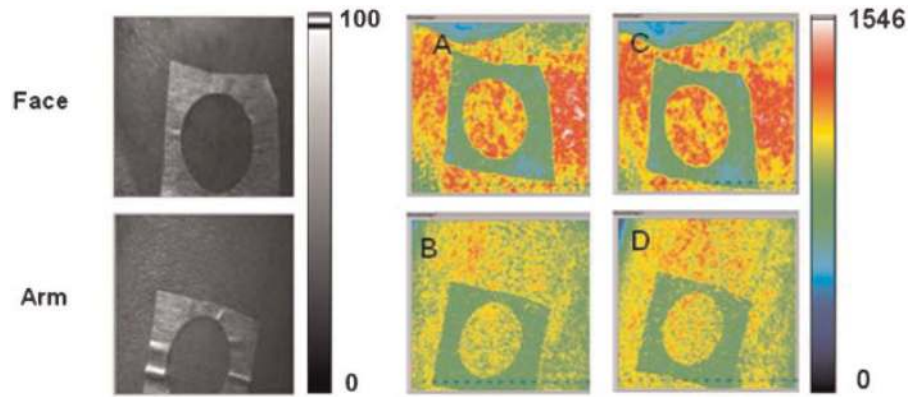


**Fig. 5.** Representative (left column) white light and (middle and right columns) SFI images taken from one of the subjects. The top row shows images taken from a region of interest on the face, and the bottom row shows images taken from a region of interest on the arm. For each row, the images taken before (**A,B**) and after (**C,D**) were similar in appearance. [Figure can be viewed in color online via [www.interscience.wiley.com](http://www.interscience.wiley.com).]

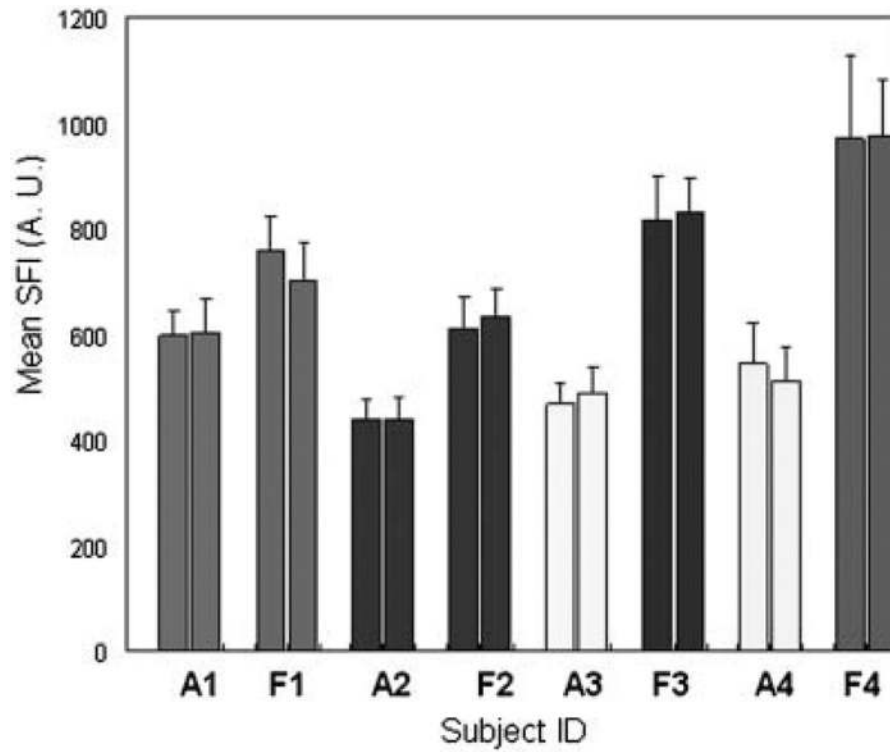


**Fig. 6.** Repeatability of SFI measurements. Each pair of vertical bars represents measurements acquired from a single site with the imaging instrument repositioned between measurements. (A) and (F) represent measurements that correspond to an arm and face, respectively.

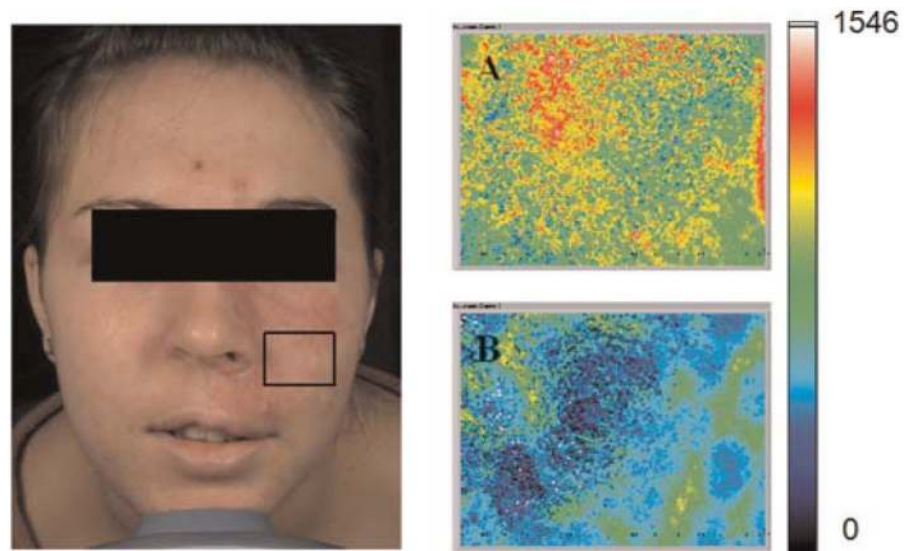


**Fig. 7.** Left: Photograph of Caucasian female patient with a PWS involving the V2 dermatomal distribution. SFI images taken from the marked region of interest in (A) immediately before and (B) 15 minutes after laser therapy. [Figure can be viewed in color online via [www.interscience.wiley.com](http://www.interscience.wiley.com).]



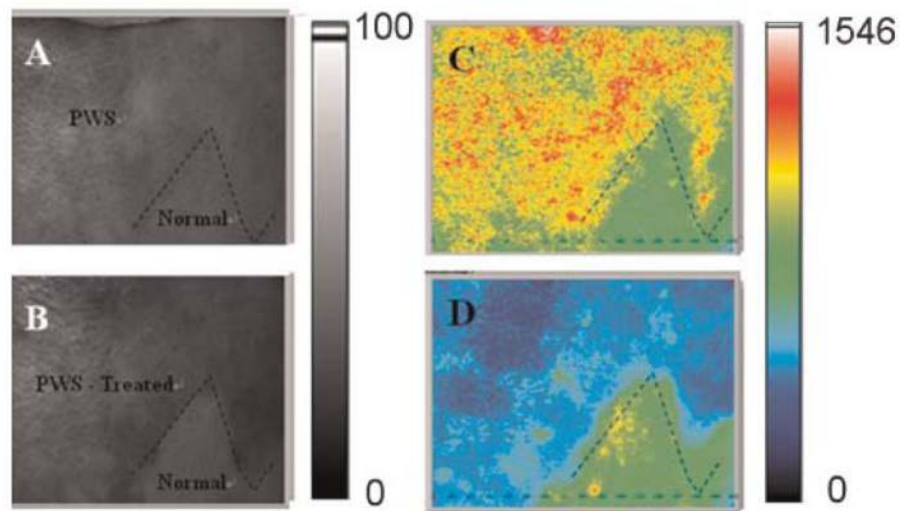
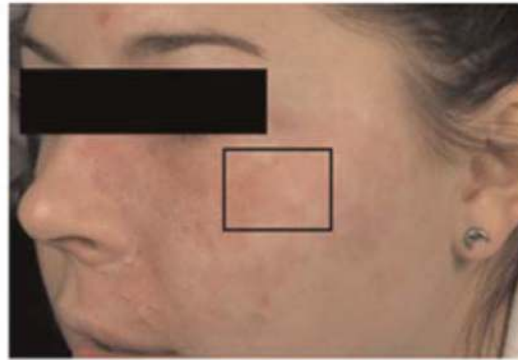


**Fig. 8.** Region of interest selected for LSI. The region was selected to include both PWS and normal skin. SFI maps (**C,D**) of a selected skin area treated with a pulsed dye laser. Parts (**A,B**) are gray scale images. Images were acquired (**A,C**) immediately before and (**B,D**) 15 minutes after treatment. The black dashed line represents the border between PWS and normal skin. [Figure can be viewed in color online via [www.interscience.wiley.com](http://www.interscience.wiley.com).]